Title

ELASTIC SCATTERING OF ANTIPROTONS ON CARBON AT 30 TO 200 Mev

Permalink

https://escholarship.org/uc/item/77s9j045

Authors

Agnew, Lewis E.
Elioff, Tom
Fowler, William B.
et al.

Publication Date

1958-04-01

UNIVERSITY OF CALIFORNIA

Radiation Laboratory

BERKELEY, CALIFORNIA

DISCLAIMER

UCRL-8285

UNIVERSITY OF CALIFORNIA

Radiation Laboratory
Berkeley, California

Contract No. W-7405-eng-48

ELASTIC SCATTERING OF ANTIPROTONS ON CARBON AT 30 TO 200 Mev

Lewis E. Agnew, Jr., Tom Elioff, William B. Fowler, Louis Gilly,
Richard Lander, Larry Oswald, Wilson M. Powell, Emilio Segrè,
Herbert M. Steiner, Howard S. White, Clyde Wiegand,
and Tom Ypsilantis

April, 1958

[illegible]

ELASTIC SCATTERING OF ANTIPROTONS ON CARBON AT 30 TO 200 Mev

Lewis E. Agnew, Jr., Tom Elioff, William B. Fowler, Louis Gilly,
Richard Lander, Larry Oswald, Wilson M. Powell, Emilio Segrè,
Herbert M. Steiner, Howard S. White, Clyde Wiegand,
and Tom Ypsilantis

Radiation Laboratory
University of California
Berkeley, California

April, 1958

In a previous letter we have reported preliminary results of measurements of the antiproton-proton elastic-scattering cross section at energies ranging from 30 to 200 Mev (lab).[1] The antiproton interactions were observed in a 30-inch-long liquid propane bubble chamber. Further measurements have yielded information on the antiproton-carbon scattering cross section for scattering angles of 5° (lab) or more. A typical $\bar{p}$-C scattering event is shown in Fig. 1.

We have seen a total of 70 antiproton-carbon scattering events in a total antiproton path length of 179 meters of liquid propane (density = 0.42 g/cm^3). In order to get an estimate of the true number of scattering events, we have multiplied the observed number by a correction factor to compensate for scanning inefficiency. This correction factor, which has been determined empirically, is about 1.7 at a scattering angle of 5°, 1.2 at 10°, and 1.1 at 20°. Scattering events at less than 5° were excluded because the scanning inefficiency becomes very large for these small angles. Although we cannot distinguish $\bar{p}$-C scatterings from $\bar{p}$-p scatterings for angles less than 7.5° because the energy of the recoil proton in $\bar{p}$-p scattering becomes too small to make a visible track, the contributi from $\bar{p}$-p scattering to our measured $\bar{p}$-C scattering in the region 5° to 7.5° is negligible.

In Fig. 2 we show the corrected $\bar{p}$-C elastic scattering cross section as a function of antiproton energy. The p-C cross sections reported by Dickson and Salter[2,3] are also shown for comparison.

The differential scattering cross section per unit solid angle as a function of scattering angle is shown in Fig. 3. Here we make no attempt to group the events according to scattering energy because of the limited number of events; consequently, this differential cross section represents an average over antipro energies ranging from [illegible]. The average [illegible] elastic $\bar{p}$-C cross section [illegible] this energy range [illegible]

In Fig. 3 we have also plotted the results of an optical-model calculation by Bjorklund and Fernbach for 140-Mev antiprotons on carbon.[4] The proton-carbon scattering measurements by Dickson and Salter[2] at 135 Mev are also shown. The optical-model potential used by Bjorklund and Fernbach is

$$V = -(V_{CR} + iV_{CI})\,\rho(r) + (V_{SR} + iV_{SI})\left(\frac{\hbar}{\mu c}\right)^2 \frac{1}{r}\,\frac{d\rho}{dr}\,\vec{\sigma}\cdot\vec{L},$$

where

$$\rho(r) = \left\{1 + \exp\left[\frac{r-R_0}{a}\right]\right\}^{-1}, \quad V_{CR} = -15 \text{ Mev}, \quad V_{CI} = 65 \text{ Mev}, \quad V_{SR} = 3.3 \text{ Mev},$$

$$V_{SI} = 1.8 \text{ Mev}, \quad a = 0.65 \times 10^{-13} \text{ cm}, \quad R_0 = 1.25\, A^{1/3} \times 10^{-13} \text{ cm}.$$

The values of the well-depth parameters were derived from the phase shifts obtained from the Ball-Chew model for nucleon-antinucleon scattering;[5] Coulomb effects are also included. The connection between the Ball-Chew phase shifts and the potentials was obtained by Drs. Geoffrey Chew and Kenneth Watson following a method of Riesenfeld and Watson.[6] From Fig. 3 one can observe (outside the Coulomb region) the large forward scattering that is present in the $\bar{p}$-C case and absent in the p-C scattering. This is interpreted as the diffraction scattering corresponding to the large total cross section of the antiprotons, and is related to the large value of V_{CI} for antiprotons in the optical model. As a comparison, if one makes a black-disk calculation, taking the radius of the disk as $\sqrt{\frac{\sigma_{abs}}{\pi}}$ and the absorption cross section as approximately 500 mb, the first minimum occurs at $\theta \simeq 22^{\circ}$, in agreement with the optical-model calculation.

In conclusion, we remark that the high ratio of the total antiproton cross section to the total proton cross section that has been observed at higher energies on several elements also extends to the lower energies considered here. These results and also details of the antiproton annihilation process in carbon will be presented in a later paper, as soon as the analysis of all events is completed.

We wish to thank Drs. Bjorklund and Fernbach for communicating to us their unpublished results, and Drs. Chew and Watson for instructive discussions.

References

1. Agnew, Elioff, Fowler, Gilly, Lander, Oswald, Powell, Segrè, White, Wiegand, and Ypsilantis, UCRL-8231 and Phys. Rev. (in press).
2. J. M. Dickson and D. C. Salter, Nuovo cimento 6, 235, 1957.
3. J. M. Dickson, private communication.
4. F. Bjorklund and S. Fernbach (UCRL, Livermore), private communication.
5. J. Ball and G. Chew, Phys. Rev. 109, 1385 (1958).
6. Riesenfeld and Watson, Phys. Rev. 102, 1157 (1956).

Figure Captions

Fig. 1. $\bar{p}$-C Scattering. The antiproton (denser track) enters from the top and left of center. At an energy of ~65 Mev, the antiproton scatters 28° to its left and continues for 7.9 cm to the lower center of the picture, where it annihilates within a carbon nucleus. The visible products of the annihilation are three π^- and two π^+ mesons.

Fig. 2. Elastic scattering cross sections.

× for $\bar{p}$-C, as a function of antiproton energy (for $\theta_{lab} \geq 5^{\circ}$)

△ for p-C, as a function of proton energy (for $\theta_{lab} \geq 5^{\circ}$)

Fig. 3. Differential scattering cross section as a function of θ_{lab}.

------ $\bar{p}$-C scattering ($200 \geq E_{\bar{p}} \geq 30$ Mev) (observed histogram)

——— $\bar{p}$-C scattering (Histogram corrected for scanning inefficiency)

-·-·-·- $\bar{p}$-C optical model calculation ($E_{\bar{p}} = 140$ Mev) by Bjorklund and Fernbach

- - - - p^+-C scattering ($E_{p^+} = 135$ Mev) by Dickson and Salter.

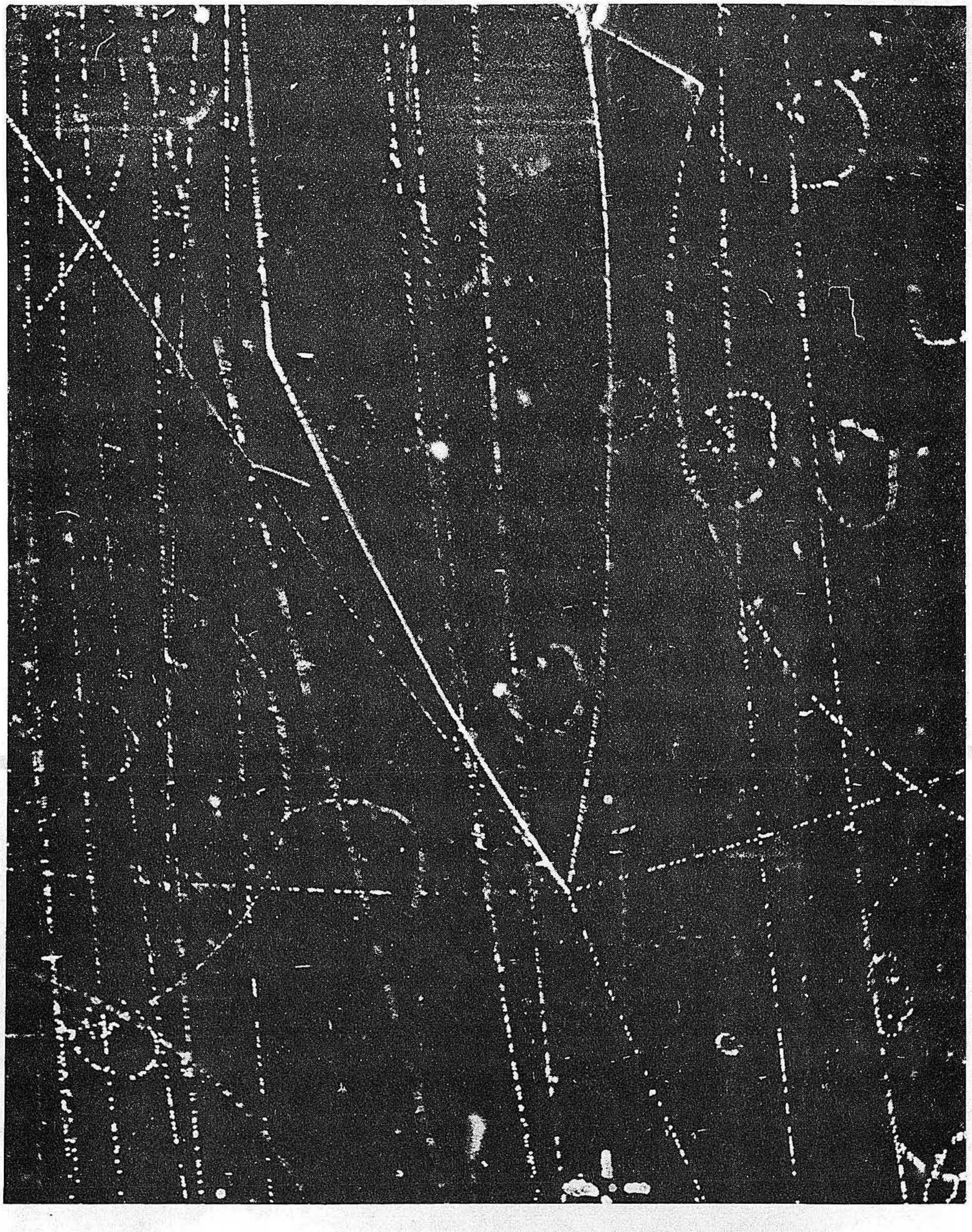

ZN-1934

Fig. 1

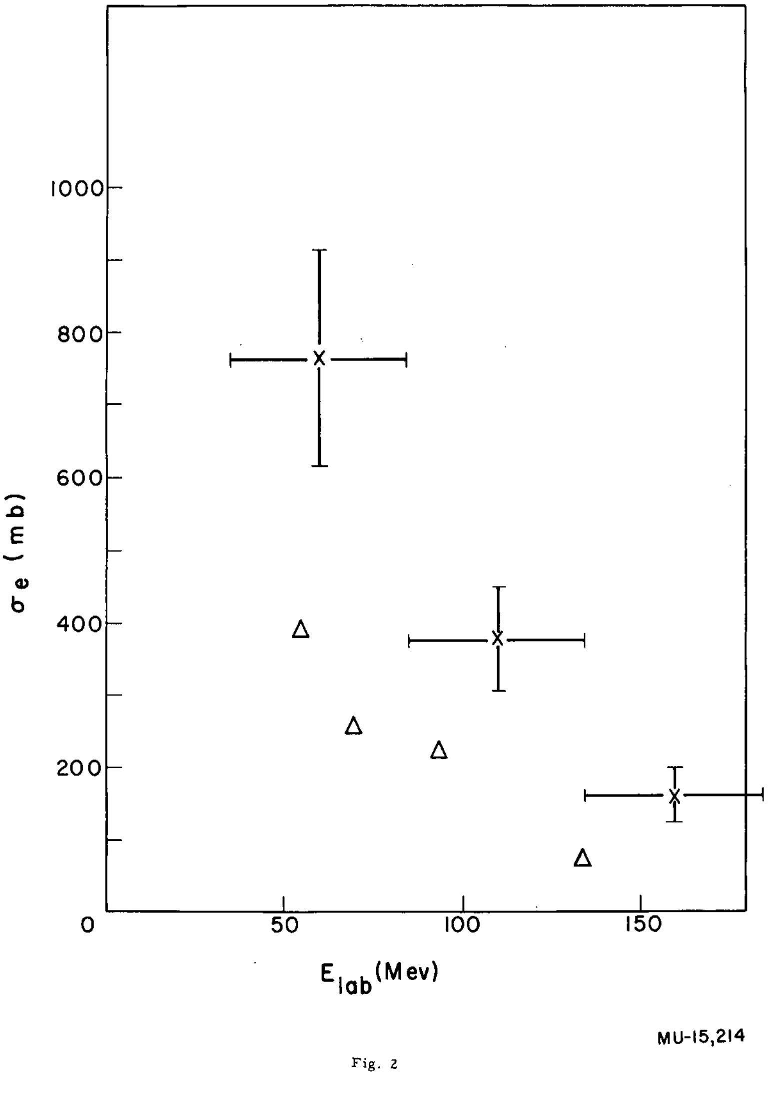

MU-15,214

Fig. 2

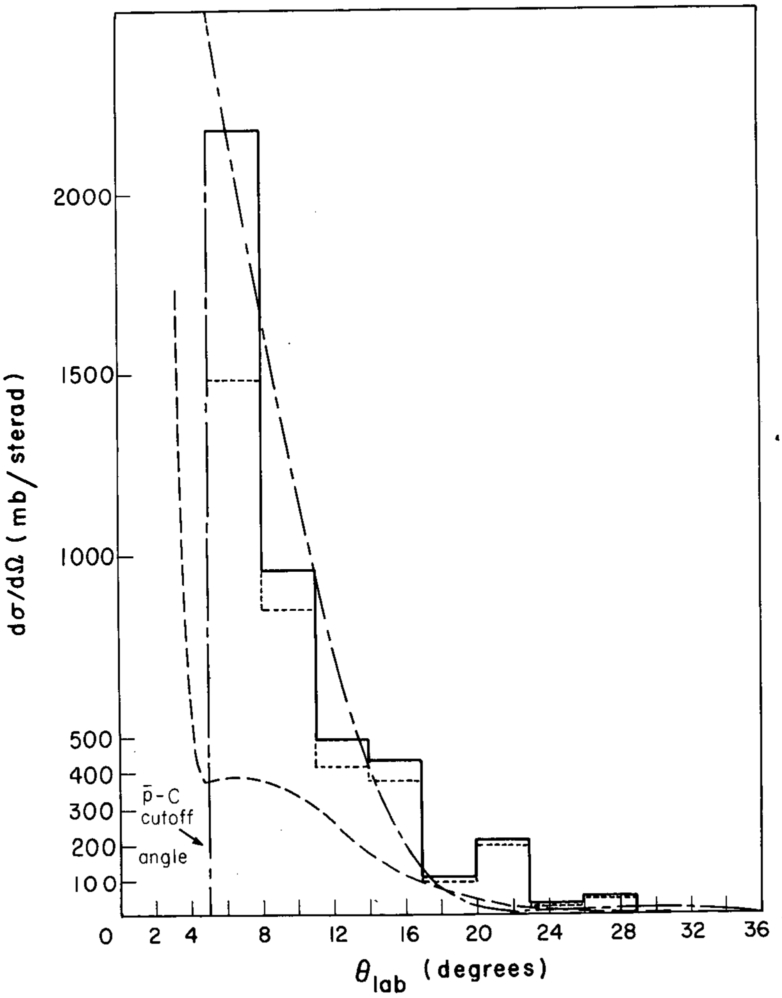

Fig. 3

MU-15,215